1-1-2010

Monitoring electric field induced changes in biological tissue by using ultrasound

Ozkan Doganay
Ryerson University

Monitoring Electric Field Induced Changes in Biological Tissue by Using Ultrasound

by

Ozkan Doganay

Physics, Ege University, 2007

A thesis

presented to Ryerson University

in partial fulfillment of the

requirements for the degree of

Master of Science

in the Program of

Biomedical Physics

Toronto, Ontario, Canada, 2010

I hereby declare that I am the sole author of this thesis.

I authorize Ryerson University to lend this thesis to other institutions or individuals for the purpose of scholarly research.

I further authorize Ryerson University to reproduce this thesis by photocopying or by other means, in total or in part, at the request of other institutions or individuals for the purpose of scholarly research.

Monitoring Electric Field Induced Changes in Biological Tissue by Using Ultrasound

Master of Science 2010

Ozkan Doganay

Biomedical Physics

Ryerson University

A new effect resulting from the application of an electric field to biomaterials was discovered by analyzing ultrasound echo signals. The new effect was observed in ex-vivo biological tissues such as porcine heart, muscle, fat, and liver and tissue mimicking phantoms for an electric field were on the order of a few Volt/cm. Changes in the arrival time of ultrasound echoes were processed using cross-correlation based algorithms. The gradient of shifting along the ultrasound axis showed a strain in the direction perpendicular to the applied electric field. The electric field also lead to changes in the ultrasound echo amplitude. The amount of the strain and the echo amplitude change depended on the history of the applied electric field. The new effect cannot be explained by resistive heating, piezoelectric effect, or electrostriction. It might be related to the electrokinetic effects.

Acknowledgements

I am extremely grateful to my supervisor, Dr. Yuan Xu. His guidance and support from the initial to the final level enabled me to develop an understanding of the subject. He graciously shared his knowledge with me and explained things clearly and simply.

I would like to thanks members of research committee Dr. Jahan Tavakkoli and Dr. Michael Kolios for helpful suggestions and important advice during all the committee meetings. I also would like to thanks Dr. Raffi Karshafian for being an external examiner and Dr. J. Carl Kumaradas being chair in my thesis examination.

I also would like to thank the following people for the help they gave me:

A. Worthington for his assistance with all types of technical problems,

Fellow graduate, S. Haider, E. Renziglova for cooperation in research,

Finally, I am forever indebted to my wife for her understanding, endless patience and encouragement when it was most required.

Contents

List of Symbols

μ	Electrophoretic mobility $[m^2V^{-1}s^{-1}]$
U	Electrophoretic velocity $[ms^{-1}]$
E	Applied electric field $[Vm^{-1}]$
σ	Surface charge density of the particle $[Cm^{-3}]$
η	Viscosity of the medium $[Pas]$
ι	Debye length $[m^{-1}]$
ξ	Zeta-potential $[V]$
ε_r	Relative permittivity of the liquid
ε_o	Permittivity of a vacuum $[Fm^{-1}]$
α	Strain
d_p	Piezoelectric strain constant $[pmV^{-1}]$
κ	Electrical conductivity $[Sm^{-1}]$
ρ	Tissue density $[kgm^{-3}]$
C	Tissue's specific heat $[jkg^{-1}K^{-1}]$
k	Thermal conductivity $[Wm^{-1}K^{-1}]$
ΔS	Time shift $[ns]$
c	Speed of sound $[ms^{-1}]$

List of Figures

Chapter 1

INTRODUCTION

1.1 Introduction

The effect of the externally applied electric field can be divided into two categories depending on the properties of the applied field. One category is non-thermal affects in biomaterial such as electrokinetic effects, piezoelectric effect, electrostriction, and electrophoresis. On the other hand, there are thermal effects which are based on Joule heating within tissue.

The non-thermal effects of an electric field on biological tissues have been investigated over the past few decades by researchers using various methods. Many of them have shown morphological changes in cells due to the applied electric field. However, the mechanism of these interactions has not been fully explained yet. This is because the applied electric field can induce several mechanical changes depending on the amplitude, frequency, and duration of the electric field, and other experimental conditions. Various methods and measurement tools, such as microelectrode techniques and optical microscopy, have been used to measure the induced potential perturbations, the permit-

tivity of tissues and deformation of the cells due to the applied electric field[20]. In some reports, microscopic views of the structural changes in the cells were illustrated, including changes in the cell orientation[21] and shape[17], and cell migration[7]. Cell-cell fusion was reported for very high voltage [22].[1]

For low electric field strength and short durations, effects were investigated in cell suspension solutions and on cell pellets [8] but not in bulk tissues as far as we know. One reason is that these studies rely on the optical microscope to observe the motion or deformation of cells. Another possible reason is that cells in bulk tissues are closely packed and cannot move as freely as in the cell suspensions. Suspensions, such as particles and cells, in an electrolyte may have surface charges even when there is no external electric field applied to the electrolyte[35]. The net charges on the surface of particles in an electrolyte can be estimated by measuring the Zeta-potential[12]. For example, microbubbles used in ultrasound can be negatively charged on their surfaces[37]. In the normal situation, red blood cells are negatively charged so that they will not aggregate together[9]. One consequence of the existence of charges on the surfaces of particles or cells in an electrolyte is that the particles and the electrolyte will be affected by an electric field in various ways, which are collectively called electrokinetic effects. When a DC external E field is applied to the colloid, the charged particles and cells in the colloid can migrate along the electric field. This is called electrophoresis[15]. When the applied electric field is alternating current, the relative motion between the particles/suspensions and the surrounding medium can result in acoustic emission. This is called an electroacoustic effect. This form of electroacoustic effect has been used to characterize the colloidal to measure the Zeta potential and particle size[6]. This electroacoustic effect has also been considered for inclusion in a new ultrasound mediated imaging method[38]. In addition,

[1]The paragraph above, quoted from the introduction section of chapter 3

P. Debye predicted another form of electroacoustic effect, the generation of an electric field when an ultrasound wave propagates in the electrolyte[5].[2]

Another consequence of the surface charges of cells is that the adhesion force is influenced by varying pH. This can be monitored by atomic force microscopy[1]. Variation in the pH value alters the tensile strength and percentage extension of fiber tissues[36] and strain properties of the collagen[31]. Induced increase in pH or increase in the charge density due to injecting a small volume of acid, changes osmotic gradients leading to strain at a region of interest[34][16]. Viscoelastic contrast of a gel phantom due to spatial variations in gel pH was reported using ultrasound strain image[40].

In this thesis we investigate whether the effects of electric field on biological tissues can be observed by utilizing ultrasound echoes. Ultrasound echoes scattered from the bulk tissues are used as a probe to investigate the electric current effects. Specifically, ultrasound echo signals are acquired continuously while the transducer is fixed at one position during the application of the electric field. Ultrasound echo signals are divided into small windows and windows are analyzed to observe the changes in the arrival time and in the echo amplitude due to application of the electric field. Then, we analyze the axial strain calculated as the gradient of the shifting. We find that the amplitude and arrival time of the echo signals show some changes correlated with the duration, strength and direction of the applied electric field. Additionally, the sample expands during the application of the electric field. The percentage change of the speed of sound is small compared with the strain in tissues. We also discuss the possible mechanisms underlying these changes.

[2]The paragraph above, quoted from the introduction section of chapter 4 (written by Dr. Xu)

1.2 Non-Thermal Effects

Three phenomenas, which are closely related to the mechanical changes on a biomaterial in an electric field, have been extensively studied both theoretically and experimentally. These phenomenas are the electrokinetic phenomena, inverse piezoelectric effect, and electrostriction.

1.2.1 Electrokinetic Phenomena

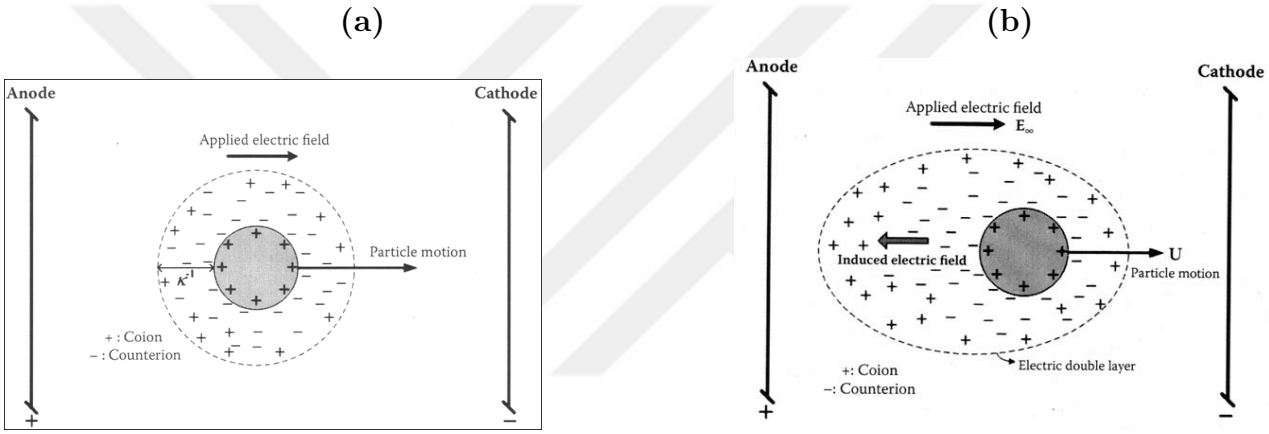

Figure 1.1: Electrophoresis of a positively charged colloidal particle due to an applied electric field.

Electrokinetic phenomena explain the interactions between a charged colloidal particle in a solution and the diffusion cloud of ions containing a net amount of charges with the opposite sign of the colloidal particle. The ionic clouds surrounds the particle is called electrical double layer as shown in Fig. 1.1 (a). The electrokinetic phenomena consists of four phenomena which are electrophoresis, electroosmosis, sedimentation potential, and streaming potential. Electrophoresis describes how a charged particle suspended in a solution moves in an applied electric field as shown in Fig. 1.1 b[15]. In the simplest case,

two forces act on the particle. One is an electric force that depends on the surface charge density of the particle, and the electric field strength. The second is the hydrodynamic friction (viscous force) that the particle undergoes in its movement through the liquid. The hydrodynamic friction depends on the viscosity of the medium, electrophoretic velocity the particle attained, and Debye length or thickness of the electrical double layer[25]. At a steady state, we define electrophoretic mobility:

$$\mu = \frac{U}{E}, \tag{1.1}$$

where U represents electrophoretic velocity of the particle (m/s), E represents the applied electric field (V/m). The term electrophoretic mobility, μ, represents a relation between electrophoretic velocity and applied electric field (m^2/Vs). It is also proportional to the surface charge density of the particle, thickness of the double layer, and the viscosity of the medium.

$$\mu = \frac{\sigma}{\eta\iota}, \tag{1.2}$$

where σ is the surface charge density of the particle(C/m^3), η is the viscosity of the medium (Pas), and ι is the Debye length or thickness of the electrical double layer(m^{-1}). Another electrophoretic mobility equation was derived with the help of the Poisson's equation.

$$\mu = \frac{\varepsilon_r \varepsilon_o}{\eta}\xi, \tag{1.3}$$

where ξ represents the Zeta-potential(V), and ε_r is the relative permittivity of the liquid, and ε_o is the permittivity of a vacuum (F/m).

Eq. 1.1, Eq. 1.2 and Eq. 1.3 explain the electrophoresis of a single isolated colloidal particle in an electrolyte solution. On the basis of these three electrokinetic equations, we

can identify the physical parameters which play an important role of the electrokinetic phenomena. These parameters are:

1) The applied electric field: electrokinetic effects are linearly proportional with the first power of the applied field. In other words, the electrophoretic response depends on the polarity of the applied electric field[6]. Additionally, the effect can be observed at a low electric field strength on the order of a few volt/cm[2][4].

2) The Zeta potential and surface charge of the particle: electrokinetic effects also depend on the surface electrical properties of the biological cells and electrical properties of the medium.

Electrophoretic mobility measurements provide information about the surface properties of biological cells since the mobility proportional to the surface charge density and Zeta-potential. Some studies show that changes in the shape of biological cells may associate with the changes in the surface charge density of cells as discussed in the introduction chapter. However, Eq. 1.1, Eq. 1.2 and Eq. 1.3 are not sufficient to make a quantitative explanation for our experimental results. These equations are derived for a single colloidal particle. Therefore, they do not include particle-particle interactions and bulk tissue properties. More complicated behavior ensues when particle-particle interactions and surface structures of a swarm of colloidal particles in concentrated suspensions are taken into account[24].

1.2.2 Inverse piezoelectric effect

Applied electric field induces a strain within a material with a certain symmetry. Some biomaterials such as collagen fibrils contain α-helix structure of polypeptide molecules. Dipoles of this molecules slightly orient with the applied electric field direction. This

mechanism is known the inverse piezoelectric effect. Mechanical strain, α, caused by inverse piezoelectric effect is roughly estimated by:

$$\alpha = d_p \times E \tag{1.4}$$

where $d_p = 2(pm/V)$ is the piezoelectric strain constant for a dry protein fiber, E is the electric field[11]. The strain has been reported on the nano-scale(10^{-9}) in a collagen fiber when an electric field applied at field strength on the order of $10^6 V/m$[30].

1.2.3 Electrostriction

An applied electric field to an anisotropic material, such as muscles, leads to the opposite sides of the domains become differently charged. Oppositely charged boundaries attracts each other, and thus material reduces thickness in the direction of the applied field. Consequently, it expands in the perpendicular direction of the applied field. The expansion of a muscle fiber caused by electrostriction is given by

$$\alpha = d_e \times E^2 \tag{1.5}$$

where $d_e = 0.3510^{-12}(m/V)^2$ is a constant proportional to radius of the muscle fiber and shear modules of the tissue. For an electric field strength of $4000V/m$, the estimated expansion in a muscle fiber is on the order of $1.1 \times 10^{-10} m$[29], and thus the strain is approximately 0.22×10^{-7}.

1.2.4 Thermal effect

The thermal effect refers to the temperature rise of the biological material caused by electric current flow in the tissue[3]. The associated Joule heating per unit volume is:

$$\dot{q} = \kappa E^2 \tag{1.6}$$

where κ is the electrical conductivity (S/m); and E represents the electric field (V/m) of the tissue. A convenient equation to estimate the temperature increase rate of the material is the bioheat equation:

$$\rho C \frac{\partial T}{\partial t} + \nabla \cdot (-k \nabla T) - \dot{q} = 0 \tag{1.7}$$

where ρ is the tissue density (kg/m^3); C is the tissue's specific heat $(j/kg.K)$; and k is the thermal conductivity $(W/m.K)$. This equation assumes that the properties of the materials are uniform.

1.3 Summary of chapters

In this chapter we briefly introduced a literature review of mechanical changes of the tissue caused by externally applied electric field. These mechanisms will be discussed in the conclusion sections of chapter 3 and chapter 4.

In chapter 2, the experimental procedures were introduced. We also discussed the computational methods to analyze changes in the ultrasound echo signals. Signal noise level was also provided.

In chapter 3, some preliminary results obtained ex-vivo experiments were presented. This chapter mostly focuses on the changes in the echo amplitude due to an electric field

application. We reported that changes in the echo amplitude and echo arrival time depend on the polarity of the applied electric field. Additionally, we ruled out Joule heating as a possible mechanism for the echo amplitude change. However, we only presented changes in a few windows.

In chapter 4 we focused on the changes in the echo arrival time on the whole sample instead of a few windows. By using shifting at the front boundary and rear boundary of the sample we investigated the strain induced of the sample. Finally, we discussed the underlying mechanisms of the induced strain considering the electrostriction, the inverse piezoelectric effect and the electrokinetic effect. This chapter concludes that the strain in the tissue can not be explained with known mechanisms that were mentioned in the first chapter.

Chapter 2

METHODS

The methods used to obtain the results reported in Chapter 3 and 4 are described in detail in chapter 3 and 4. In addition, more details on data analysis and noise level of the system are discussed in this chapter.

2.1 Experiment setup

The experimental setup is shown in Fig. 2.1. It consists of a container, function generator, an ultrasound transducer, a pulser-receiver and two data acquisition cards. The ultrasound transducer and the tissue sample were immersed in the tank filled with water or vegetable oil. Electric current was applied to the sample through embedded electrodes by a synthesized function generator (Stanford Research, model DS335). Ultrasound pulses were transmitted and received by a 10 MHz spherically-focused immersion transducer with a diameter of 1.3 cm. The focal length and the focal zone of the transducer were 1.9 cm and 0.3 cm, respectively. The transducer is connected to the ultrasound pulser-receiver (Panametrics Model 5077PR). The resulting ultrasound echo signals (A-lines)

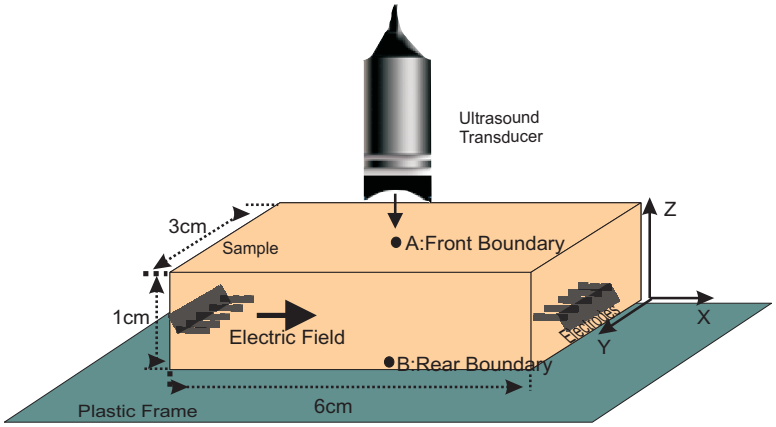

Figure 2.1: Diagram of the experimental setup.

from the sample were sampled at 200MS/s by a 14-bit CompuScope gage card, and then stored in the computer for further processing.

The tissue samples examined in the experiments were at least 6cm x 4cm x 1cm. They were positioned in a plastic frame to reduce the random mechanical motion of the sample. The top of the sample was covered with a piece of thin plastic wrap to prevent water/oil penetration into the tissues. The longest dimension and the tissue fibers were positioned perpendicular to the ultrasound beam axis. Electric current was applied to the tissue fibers through stainless steel electrodes separated by 5 cm. This arrangement gave a relatively uniform electric field inside the sample. For good coupling of acoustic waves, the tank was filled with degassed and filtered water or vegetable oil. All experiments were carried out at room temperature. Temperature was measured and recorded using a thermometer (Omegaette, HH306 DATA logger). The transducer was moved by a stepping motor (Type103-771-18, Sanyo Denki Co.). The scanning was performed along the x-axis at a step size of 0.5mm.

2.2 Experimental Protocol

The transducer was excited every 200 microseconds by the ultrasound pulser-receiver. Each A-line consists of 8192 data points and a single acquisition takes 0.5 seconds (for 500 A-line averaging). Before the electric current was turned on, 300-400 acquisitions were obtained to serve as the baseline to confirm the system stability. This baseline data also provides information about background fluctuations due to small vibrations of the experiment table and Jitter noise.

The effects of electric current on biological tissues were studied for direct current DC voltage from 2 volts to 10 volts and for alternating current (AC) from 0.02 Hz to 0.1 Hz. The resulting electric current and voltage inside the sample were measured by another two pairs of electrodes connected to the second gage card. Fresh pork heart, fat, and liver tissues from local grocery stores, and tissue mimicking gel phantoms were used as samples in the experiments.

2.3 Data Analysis

To quantify the amplitude changes and axial displacement of the arrival time (time shifting) of the collected ultrasound echo signals, each RF ultrasound echo signal was divided into small windows. Each window size is about half wavelength as shown in Fig. 2.2(a), covering one peak or one valley of the ultrasound echo signal. Using the maximum or minimum values of the window, the change in the echo amplitude within each small window was measured as a function of slow time. The slow time, is on the order of seconds as shown in Fig. 2.3, represented the instant when the ultrasound transducer was triggered and was also used to describe the time line of the application of

the voltage source to the sample. The fast time scale was on the order of microseconds and represented the arrival time of ultrasound echoes, which was the interval between the triggering of ultrasound transducer and the time echoes were received. The fast time is related to the thickness of the sample in the z axis in terms of the travel time of the ultrasound echo from the sample.

The time shifting of each window of the echo signal were also analyzed using the same windows. In this case, the shifting is calculated using cross correlation (CC) method. Thus, the shifting for all the windows in the whole sample at a time instant is obtained as a function of the fast time as shown in Fig. 2.4. Therefore, the strain in the sample was measured from the gradient of the shifting profile.

2.3.1 Measurement of the time shift using the Cross-correlation method

The Cross correlation (CC) is a method for determining the time displacements between two signals. Cross correlation f and g is defined as;

$$(f \star g)(t) = \int f(\varepsilon) \times g(\varepsilon + t)\, \mathrm{d}\, \varepsilon \tag{2.1}$$

This integration determines how much the function g must be moved along the time to be aligned with f. f and g functions in a window of an ultrasound echo signal is shown in Fig. 2.2(a). ΔS represents the displacement in the arrival time or the shifting between f and g functions. Eq. 2.1 can be easily implemented in Matlab by the convolution theory. The convolution theory provides a connection between the f and g functions and

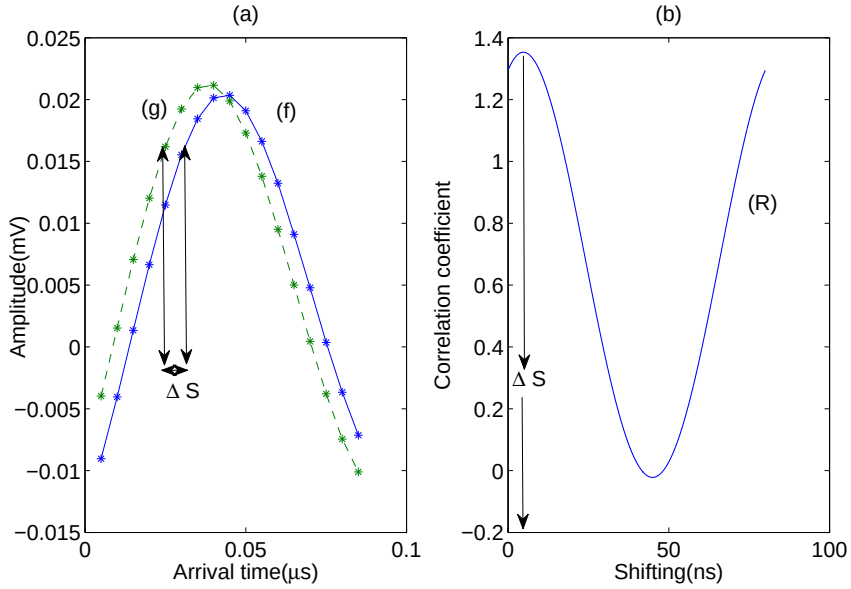

Figure 2.2: Example of shifting estimation in a window (a) Shifting, ΔS, between the ultrasound echoes f and g in a window. Stars represent data points. (b) R represents correlation of f and g.

their Fourier transform F and G [28]. The convolution theory was defined by:

$$(f * g)(t) = \int f(\varepsilon) \times g(t - \varepsilon)\, \mathrm{d}\, \varepsilon = \mathfrak{F}^{-1}\{F \cdot G\} \tag{2.2}$$

where $\mathfrak{F}^{-1}$ is the inverse Fourier transform. Based on, Eq. 2.2, the correlation in the spatial domain is equivalent to the inverse Fourier transform of the product of F and G^* [33]. The correlation can be given by:

$$(f \star g)(t) = \mathfrak{F}^{-1}\{F \cdot G^*\} \tag{2.3}$$

where G^* represents the complex conjugate of G. In order to increase accuracy of calculating the shifting, the data number of the f and g function can be increased using interpolation(cubic spline) function:

$$f_i = f * interpolation \; and \; g_i = g * interpolation \tag{2.4}$$

Then, the interpolated f and g are placed in Eq. 2.3

$$R = \mathfrak{F}^{-1}\{F_i \cdot {G_i}^*\} \tag{2.5}$$

where R, correlation coefficient, represents a curve as shown in Fig. 2.2(b) (it is called Cross correlation function). The maximum point of the cross correlation function is the best alignment or the highest correlation registered between the function f and g as shown in Fig. 2.2(b). Thus,

$$\Delta S = \Delta t|_{Max(R)} \tag{2.6}$$

The shifting measurement based on tracing the maximum discrete correlation have been used in many studies [23] [10]. This method only consider the shifting in the echo signal along to the direction of the beam propagation. However, experiment results shows that the echo signal fluctuates back and forth. These small fluctuations, less than 0.5ns, are thought to be background fluctuations. If the shifting of the consecutive echoes decreases to a very small value, the point of the maximum correlation will show a big variation. Although the background fluctuations are very small, on the order of 0.5ns, they cause a big noise in the shifting estimation, on the order of 150ns. This noise is shown in Fig. 2.3(b) and (e). The noise associated with the background fluctuations can be eliminated as shown in Fig. 2.3(c) and (f).

This method can be used to determine the shifting or the time displacements in the ultrasound echo signal accurately depending on number of interpolation as shown in Fig. 2.3. Fig. 2.3(a) and Fig. 2.3(d) show shifting which is computed without interpolation. In this case, the highest accuracy of the measurement is on the order of $5ns$ (the inverse of the sampling frequency of the RF signals), which limits the measurement of the shifting smaller than $5ns$. However, a measurement of the shifting on the order of $0.5ns$ nanoseconds is possible using the interpolation as shown Fig. 2.3(c).

2.3.2 Measurement of the expansion and strain

Strain refers to the amount of elongation in the sample experiences compared to its original size in the ultrasound wave propagation axis or z-axis as shown Fig. 2.1. For example, the sample's first length is $L = 1cm$ on the z-axis side and than it expands and becomes 1.001cm long. Thus, the strain is calculated $\alpha = \Delta L/L = 0.001cm/1cm$ or 0.001 where ΔL represents the induced change of L. The strain is sometimes expressed

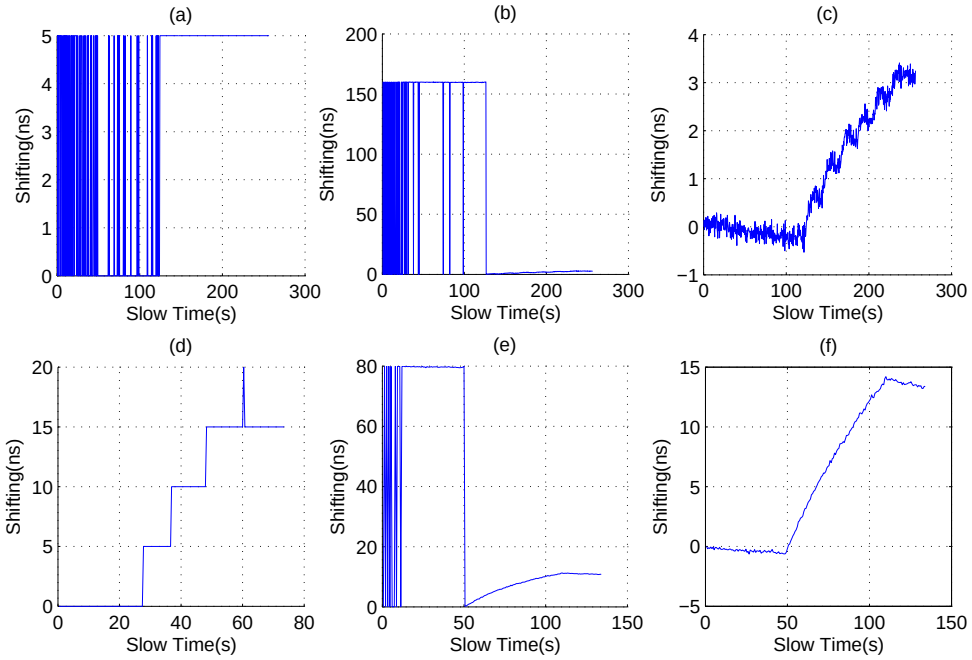

Figure 2.3: (a)Estimation of a small shifting without interpolation; (b) after interpolation; (c) after filtering the noise. (d) Estimation of a big shifting without interpolation; (e) after interpolation; (f) after filtering the big noise.

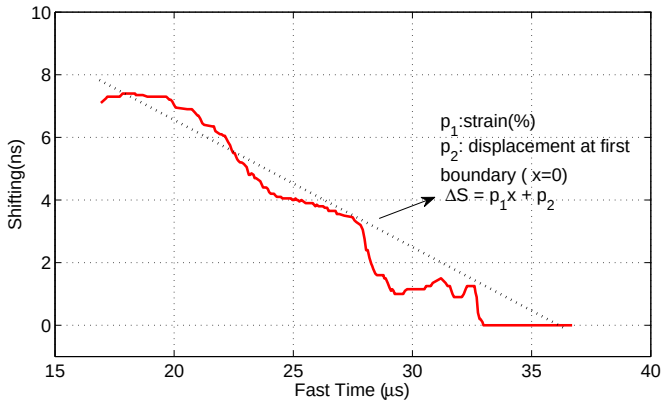

Figure 2.4: Solid line represents time shifting along the ultrasound propagation axis, doted line represents liner fitting

in percent, so the percentage strain is $p_1 = 0.1\%$. In this study the strain was calculated on the scale of fast time or arrival time.

The time shifting is calculated for each window along the ultrasound propagation axis, giving information about the shifting gradient of the whole sample at a time instant as shown in Fig. 2.4. The axial strain was calculated as the gradient of the shifting by implementing linear regression technique [27] [23]. The percentage strain, displacement of the first boundary and rear boundary were obtained from the linear regression:

$$\Delta S = p_1 \times x + p_2 \tag{2.7}$$

where p_1 is the percentage strain in the sample, p_2 represents displacement ΔS at the first boundary for $x = 0$. Displacement at the rear boundary can be also calculated with the help of Eq. 2.7 for $x = L$. ΔL refers to $\Delta S \times c/2$, where c is the speed of sound. Thus, a time series of percentage strain (creep) of the sample was generated by repeating this analysis for each data.

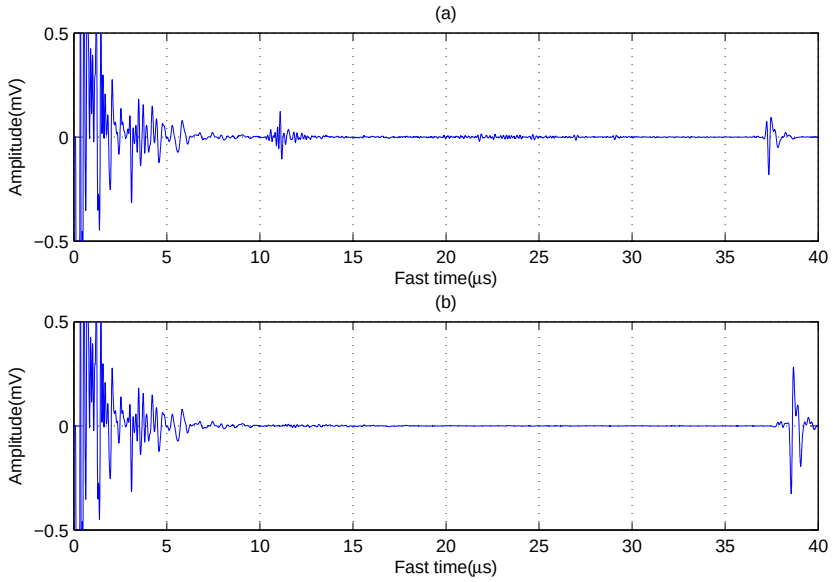

Figure 2.5: Pulse Echo response along the z axis in the experiment set up, (a)with the sample, or (b)without the sample.

2.4 Noise Level

Two RF signals, obtained with and without the sample, in Fig. 2.5, were obtained from the experiment setup as shown in Fig. 2.1. To investigate the noise in the echo signal, the signal with the sample was compared with the signal with the coupling medium (without the sample). Fig. 2.5(a) shows the first and rear boundary at the sample. The segment of the signal from $0\mu s$ to $10\mu s$ represents the interval between the transducer and sample. The strong signal that occurs in this interval are related to the interference due to the firing of the transducer. These artifacts can not be considered as noise, since they are stationary and repeatable. However, they are independent of the sample. Their magnitudes are larger than the random noise and decay gradually as when the arrival time (equivalently deeper inside the sample) increases, as shown in the comparison between

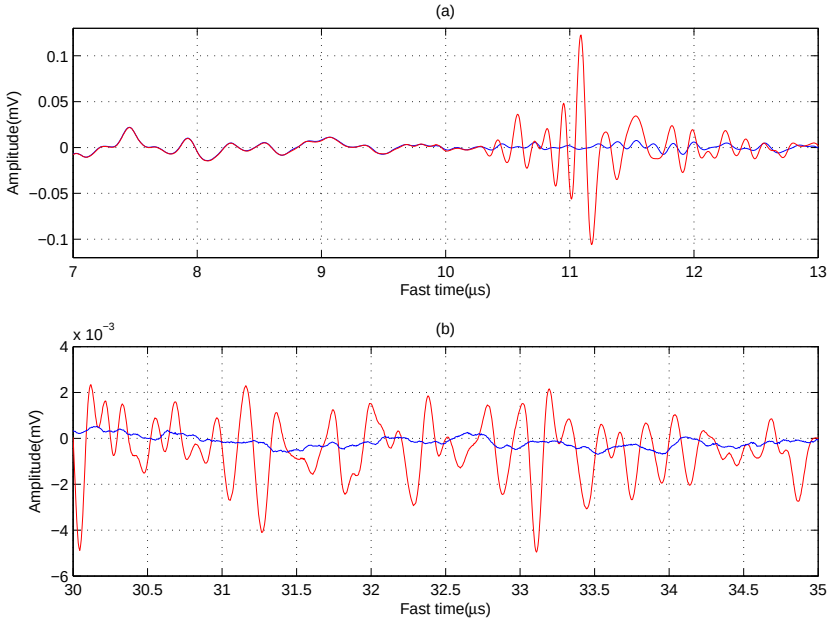

Figure 2.6: A segment of the Pulse Echo response with and without sample are compared, (a) near the first boundary, and (b)near the rear boundary.

Fig. 2.6 (a) and (b). Therefore, we'll compare the echoes from the sample with these artifacts to obtain an equivalent SNR.

In Fig. 2.6, a small segment of the signal from tissue and from the coupling medium alone are compared to each other. The signal between $7\mu s$ and $10\mu s$ is stationary and repeatable. Other than this interval, signal amplitude from tissue is always longer than the artifact. The interval in Fig. 2.6(c) shows the smallest signal amplitude, occurring near the rear face. In this segment of data, the peak to peak value of the signal from tissue is approximately $6 \times 10^{-3} mV$ and from the coupling medium $1 \times 10^{-3} mV$. Thus, the signal noise ratio is approximately $y = 6$ and the dB ratio, L_p, is given by:

$$L_p = 20 \times \log y = 15.6 dB \tag{2.8}$$

Hence, the artificial fluctuations are negligible compared with the signal from sample.

The main source of noise in the measurement of the shifting and strain is the base line fluctuations. This fluctuations are caused by vibrations in the experiment setup and the error due to the delay-estimation algorithms as shown in Fig. 2.6 (c) (between $0s$ and $100s$). The vibrations in the experiment setup can be reduced by immobilizing the transducer and sample; however, Jitter noise still limits the small shifting measurements that less than a few nanoseconds. The error due to the delay-estimation algorithms depend on many factors including the step size of the convolution and windowing size. The error due to the delay-estimation algorithms in the shifting measurements can be reduced as shown in Fig. 2.6 (a) and (d) by interpolation of the raw RF data. Eventually, the noise level in the shifting data is on the order of $0.5 - 2ns$ depending on the experimental conditions. It always can be observed in the base line interval and is negligible for shifting on the order of $10 - 15ns$ as shown in Fig. 2.6 (d).

Chapter 3

RESULTS I

3.1 THE EFFECT OF ELECTRIC CURRENT ON BIOLOGICAL TISSUES

3.1.1 Abstract

The amplitude and phase changes of ultrasound echoes from biological tissues are investigated when a physiological level (2.0V/cm) of DC or extremely low frequency AC electric field is applied to the tissues. Ultrasound echo signals were acquired continuously during the application of the electric field with the transducer fixed at one position. Some small windows are chosen in the ultrasound signals. The peak-to-peak values of the signals are used as the amplitudes and the flight times are used to represent the phases in each individual window. Experimental results show that the amplitude changes and the phase shifts of the echo signals are correlated with the applied electric current. [3]

[3]This work presented in this chapter was presented at the IEEE Ultrasonics Symposium (2009) and published in IEEE proceedings

3.2 Introduction

The effects of electric field on biological tissues have been investigated over the past few decades by researchers with various methods. Many of them have shown morphological changes in cells due to the applied electric field. However, the mechanism of these interactions has not been fully explained yet. This is because the applied electric field can induce several mechanical changes depending on the amplitude, frequency, and duration of the electric field, and other experimental conditions. Various methods and measurement tools, such as microelectrode techniques and optical microscopy, have been used to measure the induced potential perturbations, the permittivity of tissues and deformation of the cells due to the applied electric [20]. In some reports, microscopic views of the structure changes in the cells were illustrated [17][8][13], including changes in the cell orientation and shape, cell rotation, and cell movement. Cell-cell fusion was reported for very high voltage [41][22]. For low electric field strength and short durations, effects were investigated in cell suspension solutions and on cell pellets because of the difficulties in detecting small changes [41][21][19][18][26]. Optical microscopes were used in all of the above studies, thereby only the changes in the surface layer of the sample could be monitored.

In the present study we investigate whether the effects of electric field on biological tissues can be observed by utilizing ultrasound echoes from the biological tissues. Specifically, ultrasound echoes scattered from heart and muscle are used as a probe to investigate the electric current effects. Results show that the amplitude and phase of the echo signals show some repeatable changes correlated with the duration, strength and direction of the exposed electric current. This new technique may be useful for observing the morphological responses of biological tissues to low intensity and low frequency elec-

tric fields in vivo. Compared with the optical microscope technique, it has the advantage of providing in-depth information on the electric changes in biological tissues induced by electric field. This technique can also potentially provide a new contrast mechanism for ultrasound imaging.

3.3 Methods

In order to study the effect of electric field on ultrasound echoes from biological tissue, the ultrasound echo signals were acquired continuously during the application of the electric field with the transducer fixed at one position. Some small windows are chosen in the ultrasound signals. The peak-to-peak values of the signals are used to represent the signal amplitudes and the flight times of peaks are used to represent the phases in each individual window. The amplitudes and flight times in some windows are plotted as a function of time for duration of several minutes.

3.3.1 Experimental Setup

The experimental setup is shown in Fig. 3.1. It consists of a container, function generator, an ultrasound transducer, a pulser-receiver and two data acquisition cards. The ultrasound transducer and the tissue sample were immersed in the tank filled with water or vegetable oil. Electric current was applied to the sample through embedded electrodes by a synthesized function generator (model DS335). Ultrasound pulses were transmitted and received by a 10 MHz spherically-focused immersion transducer with a diameter of 1.3 cm. The focal length and the focal zone of the transducer were 1.9 cm and 0.3cm, respectively. The transducer is connected to the pulser-receiver (Panametrics Model 5077PR). The resulting ultrasound echo signals (A-lines) from the sample were sampled

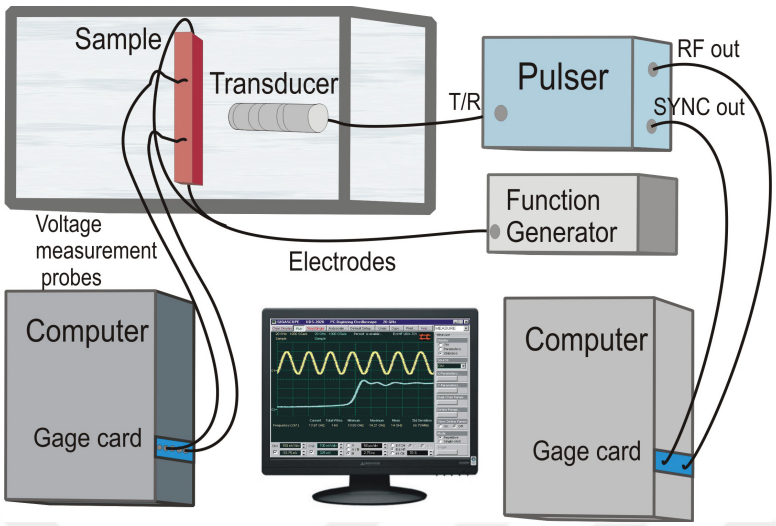

Figure 3.1: Diagram of the experiment setup.

at 200MS/s by a 14-bit CompuScope gage card, and averaged 2500 times and then stored in the computer for further processing.

The tissue samples examined in the experiments were at least 6cm x 4cm x 1cm. They were positioned in a plastic frame to reduce the random mechanical motion of the sample. The top of the sample was covered with a piece of thin plastic wrap to prevent water/oil penetration into the tissues. The longest dimension and the tissue fibers were positioned perpendicular to the ultrasound beam axis. Electric current was applied to the tissue fibers through stainless steel electrodes separated by 5 cm. This arrangement gave a relatively uniform electric field inside the sample. For good coupling of acoustic waves, the tank was filled with degassed and filtered water or vegetable oil. All experiments were carried out at room temperature.

3.3.2 Experimental Protocol (Data Acquisition)

The transducer was exited every 200 microsecond by the pulser-receiver. Each A-line consisted of 8192 data points and a single acquisition took 3.75 seconds due to the averaging. Before the electric current was turned on, 300-400 acquisitions were obtained to serve as the baseline to check the system stability. This interval also provides information about background fluctuations due to small vibrations of the building and the experiment table. The effects of electric current on biological tissues were studied for DC voltage of 10 volts and for 0.025Hz alternating current (AC). The resulting electric current and voltage inside the sample were measured by another two pairs of electrodes connected to the second gage card.

3.3.3 Data Analysis

To quantify the amplitude and phase changes of the collected echo signals, windows were chosen in the A-mode signal as shown in Fig. 3.2. Each window size is about one wavelength, covering one peak and one valley of the echo signal. Using the maximum and minimum values of the each window, the amplitude was obtained and plotted versus time in Fig. 3.3. Phase changes of the signal were also analyzed using the same window. In this case, the flight time of the peak in the window is plotted as a function of time (Fig. 3.4). The first time derivative of the amplitude data was compared with the voltage inside the sample as shown in Fig. 3.5. To eliminate the background fluctuation of the amplitude for taking the derivative, the data was smoothed using the Lowess method (Locally weighted scatter plot smooth using linear least squares fitting and a first-degree polynomial) before the derivative.

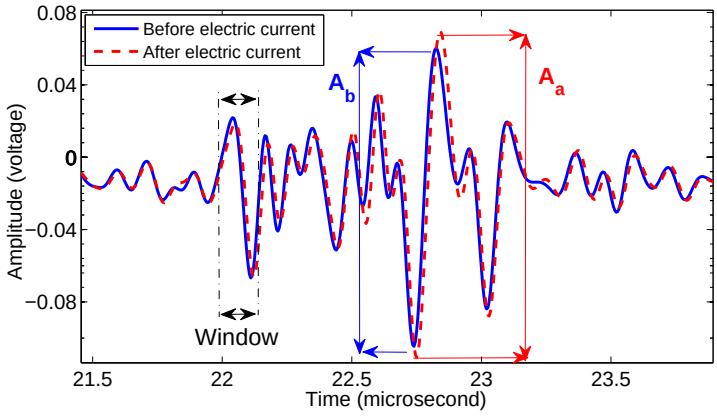

Figure 3.2: The echo signals from a piece of bovine muscle tissue before electric current application, after 10V and after -10V application were compared.

3.4 Results

Fig. 3.2 shows part of the ultrasound echoes from a piece of bovine muscle before (solid line) and after (dotted line) applying a DC voltage of 10 Volts for 40 seconds to the tissue. A_a and A_b denote the peak-to-peak value of the signal within a small window after and before the application of the electric field to the tissue, respectively. They are used to represent the amplitude of the signal within the window. After the application of the electric field, the amplitude increases in some windows and decreases in others and the arrival time of the signal are delayed, by approximately 26 ns, in the selected window. The magnitude and sign of the change in the amplitude and arrival time in different windows are different, as shown in Fig. 3.3 and Fig. 3.4.

One possible of explanation of the amplitude change and shifting of the signal is Joule heating due to the electric current in a resistive medium. Joule heating can increase the temperature of tissue. The change in ultrasound signal, especially the time shifting, has been studied extensively in strain imaging. Temperature increase can change the

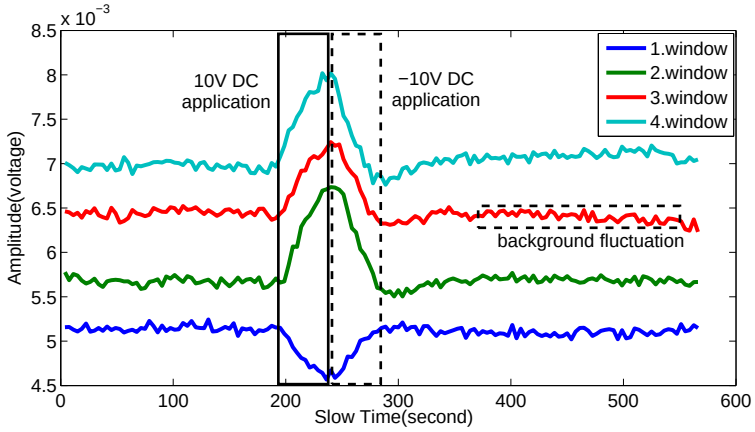

Figure 3.3: Peak-to-peak amplitude in 4 windows of echo signals from a pork heart tissue. Positive (in solid rectangle) and negative (in dashed rectangle) DC voltage were applied for 45 and 48 seconds, respectively.

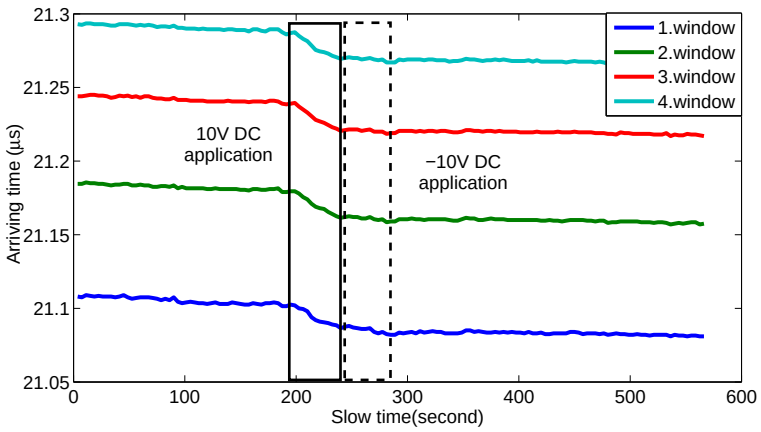

Figure 3.4: The peak positions in four windows of the echo signals from a piece of pork heart tissue. Positive (in the solid rectangle) and negative (in the dashed rectangle) DC voltages were applied for 45 and 48 seconds, respectively.

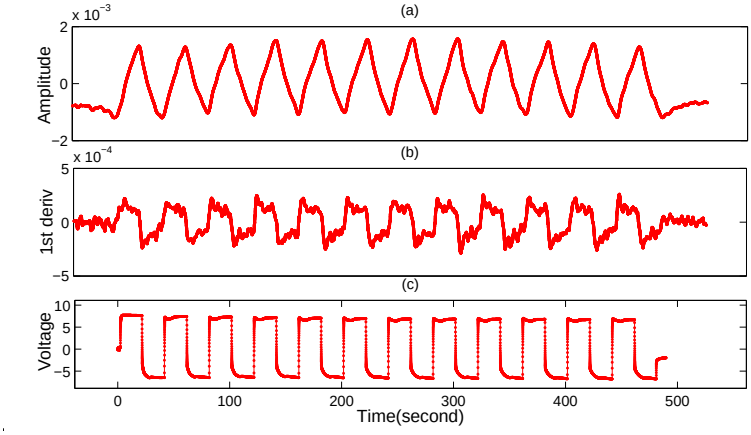

Figure 3.5: (a) The amplitude of the ultrasound backscattered signal in a window versus time when an AC voltage was applied. (b) Derivative of the response gives the applied wave form. (c) Measured potential difference inside the sample during the current application.

ultrasound backscattering coefficient of the tissue, and consequently the amplitude of the ultrasound signal. Temperature increase can also induce the time shifting of the ultrasound signal through thermal expansion and the change of the acoustic speed in the tissue.

To investigate if the amplitude change and shifting of the signal is due to Joule heating, we apply two DC voltages with the same amplitude and duration but opposite polarity sequentially to a pork heart tissue. The amplitudes in four windows of the echo signal are plotted as a function of time in Fig. 3.3. Every 3.75 seconds, one echo signal from the pork heart tissue was recorded. Before current application, the interval from 0 to 190 seconds gives the information about the system stability and the background fluctuation. During this time interval the background fluctuation of the amplitude was measured to be approximately 1.5% of the amplitude. The intervals of the exposures to the DC electric field are marked by two rectangles. First, the solid rectangle indicates positive 10 volt DC application for 45 seconds. The second rectangle (dotted line),

defines the negative 10V for 48 seconds. Upon the current application, the amplitude of the signal increased sharply in some windows and decreased in other windows as shown in Fig. 3.2. When DC voltage polarity was reversed, the direction of changes in the amplitude was also reversed, suggesting some directionally dependent changes. When the two DC applications have the same voltage and duration but opposite signs, the amplitudes also return to the same level as before the application of the electric field. This suggests that the amplitude change induced by the current application is sensitive to the polarity of the applied electric field and the amplitude change is reversible. We conclude that some reversible changes in the mechanical properties of the tissues are responsible for the amplitude change in the ultrasound echoes. This result excludes Joule heating as a possible mechanism for the amplitude change, because Joule heating is independent of the direction of the electric field. The rate of the temperature increase for 10V application in the muscle tissue is estimated to be $1.5 \times 10^{-3\circ} C/s$. The temperature increase with one minute current application is less than 0.1 degree and cannot explain the up to 15% amplitude change observed in the experiments.

The relation between the applied DC field and the shifting response in the 4 windows are illustrated in Fig. 3.4. Similar to the amplitude changes, sharp changes in the arrival times of the signals were also observed when DC of 10V was applied to the tissue. Unlike the case of amplitude change described above, shifting did not return to original position when the opposite DC voltage was applied. However, the rate of the change of the arrival time changes when the sign of DC application changes as shown in the dotted rectangle in Fig. 3.4. To study the change of the ultrasound signals when an AC current is applied to tissues, we applied a square wave voltage [Fig. 3.5 (c)] with the amplitude of 8V and a frequency of 0.025 Hz to a sample of heart tissue. Fig. 3.5 (a) shows the smoothed amplitude of the echo in one window versus time. The amplitude of the echo changes

periodically with a triangle waveform at the same frequency as the applied voltage. Fig. 3.5 (b) shows the first time derivative of smoothed amplitude of the echo signal in Fig. 3.5 (a). Comparison of Fig. 3.5 (b) and (c) shows a strong correlation between the first derivative of the amplitude and the applied voltage. This feature of backscattered echo signal may suggest a new method to monitor the electric field in biological tissue by analyzing the ultrasound echoes from the tissues.

3.5 Conclusion and future work

It has been known for decades that electric fields induce some mechanical interactions in biological tissues. These mechanical changes of the biological tissues have been studied in various ways by several research groups experimentally and theoretically. We have introduced the ultrasound wave as a probe for observation of mechanical changes due to physiological-level electric field application. We have observed some nonrandom mechanical changes due to electric current application at field intensities 0.4V/cm and 60 second time duration.

When the polarity of the electric field is reversed, the sign of the change of the resulting amplitude is also reversed. On the basis of our present experiment results we can conclude that the amplitude changes are not a result of temperature increase. The amplitude changes are associated with a mechanic change that is sensitive to the direction of the applied electric field in tissues.

One of the future studies is to determine the dependence of the amplitude and phase change in the ultrasound echo on the amplitude, frequency, and duration of the applied current quantitatively. In addition, images of the amplitude and phase changes in the ultrasound signals due to the applied electric field may provide further information for

probing biological tissues and understanding the underlying mechanisms.

Chapter 4

RESULTS II

4.1 ELECTRIC-FIELD INDUCED STRAIN IN BIOLOGICAL TISSUES

4.1.1 Abstract

This paper reports a new effect whereby a physiological-level direct-current electrical field (at 1.4V/cm) can induce time-varying mechanical strain in various types of biological tissues and gel phantoms. This effect cannot be explained by the piezoelectric effect, tissue contraction, temperature changes, and electrorestriction. The induced strain in tissues was analyzed by processing ultrasound echo signals. The sample expanded perpendicularly to the applied electric field. The expansion rate depended on the history of the applied electric field. The speed of sound changed little compared with the expansion. The new effect might be related to electrokinetic effects.[4]

[4]This work presented in this chapter was submitted for publication to the Journal of the Acoustical Society of America(JASA) (August 10, 2010)

4.2 Introduction

Suspensions, such as particles and cells, in an electrolyte may have surface charges even when there is no external electric field applied to the electrolyte[35]. The net charges on the surface of particles in an electrolyte can be estimated by measuring the Zeta-potential[12]. For example, microbubbles used in ultrasound can be negatively charged on their surfaces[37]. In the normal situation, red blood cells are negatively charged so that they will not aggregate together[9].

One consequence of the existence of charges on the surfaces of particles or cells in an electrolyte is that the particles and the electrolyte will be affected by an electric field in various ways, which are collectively called electrokinetic effects. When a DC external E field is applied to the colloid, the charged particles and cells in the colloid can migrate along the electric field. This is called electrophoresis[15]. When the applied electric field is alternating current, the relative motion between the particles/suspensions and the surrounding medium can result in acoustic emission. This is called an electroacoustic effect. This form of electroacoustic effect has been used to characterize the colloidal to measure the Zeta potential and particle size[6]. This electroacoustic effect has also been considered for inclusion in a new ultrasound mediated imaging method[38]. In addition, P. Debye predicted another form of electroacoustic effect, the generation of an electric field when an ultrasound wave propagates in the electrolyte[5].

It has been reported that cells can change shape[17] and orientation[21] and migrate[7] in an external electric field. The above effects have been studied in colloid, blood, and cell cultures, but not in bulk tissues as far as we know. One reason is that these studies rely on the optical microscope to observe the motion or deformation of cells[8]. Another possible reason is that cells in bulk tissues are closely packed and cannot move as freely

as in the cell suspensions.

Our previous results have shown that there were mechanical changes in bulk biological tissues when they were subject to an external field, and that these changes were monitored through the changes in the ultrasound echoes from the bulk tissues[39]. These results can be considered a generalization of the reported study on cell culture applied to bulk biological tissues. In our previous study, ultrasound echo signals were acquired continuously while the transducer was fixed at one position during the application of the electric field. Some small windows were chosen in the ultrasound signals to analyze the amplitude and phase changes. The peak values of the signals were used to represent the echo amplitudes, and the arrival times of the peaks were used to represent the phases in each individual window.

In this paper, we analyze the strain induced in tissues due to the application of an electric field. We find that the sample expands during the application of the electric field. The percentage change of the speed of sound is small compared with the strain in tissues. We also discuss the possible mechanisms underlying these changes.

4.3 Experimental setup

The diagram of the experimental setup using a stand-alone single-element ultrasound transducer was shown in Fig. 1 of our previous paper [39]. It consisted of a water tank, a function generator(Stanford Research, model DS335), an ultrasound transducer (Panametrics Model V311), a pulser-receiver (Panametrics Model 5077PR), and two data acquisition cards. The transducer was a 10-MHz 70% bandwidth spherically-focused immersion type with a diameter of 1.3 cm and a focal length of 1.9 cm. The transducer is connected to the pulser-receiver. The ultrasound transducer and the sample were im-

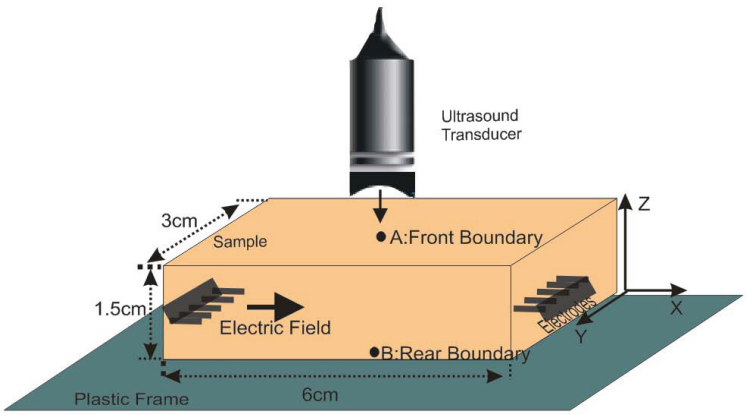

Figure 4.1: Diagram of the experimental setup.

mersed in a tank filled with (deionized) water or vegetable oil (Selection, Metro). The deionized water and vegetable oil were chosen to avoid the potential electric coupling between the transducer and the electric field inside the sample. An electric field was applied to the sample through embedded electrodes by a synthesized function generator, as shown in Fig. 4.1. Ultrasound pulses were transmitted and received by the transducer. The ultrasound echo signals (A-lines) were sampled at 200 MHz/s by a 14-bit CompuScope Gage card, averaged 2500 times, and then stored in a computer for further processing. The samples used in the experiments were about 6 cm $\times$ 4 cm $\times$ 1.5 cm.The electrodes were cut from single-row square headers. Each electrode was about 1.2 cm wide and had four pins coated with gold. Each pin was 2.54 mm thick and 5 mm long. In the experiments, we focused the ultrasound to the middle part of the sample, which has a relatively uniform current density.

4.4 Experimental protocol

All the samples of biological tissues used in this study were from local grocery stores. The data presented in this paper were obtained from the experiment on a piece of fresh porcine heart tissue. Similar experiments were also repeated in porcine muscle, kidney, liver, and fat, and gelatin phantoms (3% salt and 10% gelatin powder from pork skin (Gelatin, Sigma-Aldrich Co.)). To prevent any potential diffusion of water or oil between the sample and the coupling medium (water or oil), a very thin layer ($< 0.5mm$) of plastic membrane (Resinite packaging film, AEP Canada Inc.) was wrapped around the sample. However, the comparison between the experiments with and without the plastic membrane did not show significant difference.

Before the electric field was applied, 300-400 A-mode RF signals were acquired for about 50 seconds to serve as the baseline to check the system stability. The ultrasound signals in this interval provided information about the fluctuations in the amplitude and arrival time of the ultrasound signals due to the small vibrations of the building and the experiment table. Then we used the following experiment protocol: (1) A 7-V voltage source was applied to the sample for one minute, from $t_1 = 50s$ to $t_2 = 110s$. (2) The sample was disconnected from the voltage source for 5 minutes, from $t_2 = 110s$ to $t_3 = 445s$. (3) An identical, but opposite voltage was applied to the sample for one minute, from $t_3 = 445s$ to $t_4 = 505s$. (4) The sample was disconnected from the voltage source after $t_4 = 505s$.

Two time scales were used to plot the results. The slow time, such as the above t_1, t_2, t_3, and t_4, was on the order of seconds as shown in Fig. 4.3(a). It represented the instant when the ultrasound transducer was triggered and was also used to describe the time line of the application of the voltage source to the sample. The fast time scale was on the

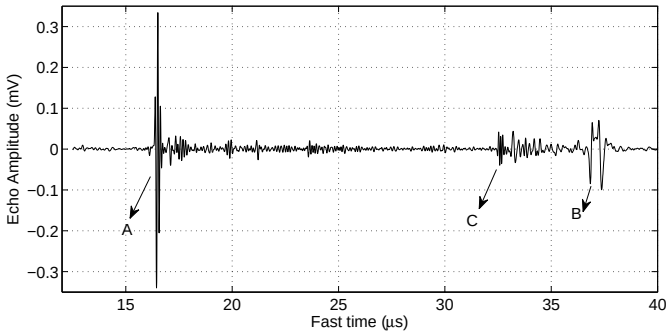

Figure 4.2: Ultrasound RF signal versus fast time, with the front and rear boundaries indicated by A and B, respectively. C represents the second echo (reverberation) from the front boundary of the tissue.

order of microseconds and represented the arrival time of ultrasound echoes, which was the interval between the triggering of ultrasound transducer and the received echoes. The fast time related to the thickness of the sample in the z axis in terms of the travel time of the ultrasound echo from the sample. The method employed to quantify the changes of the amplitude and arrival time of the RF echo signals was similar to the one used in our previous study[39]. The RF signal was divided into windows with a size of about two wavelengthes. The time-shiftings between the corresponding windows of the RF signals at two slow-time instants were analyzed with a method based on cross-correlation. The method to calculate the time-shifting will be reported in details in our future paper. In this paper, we focused on the strain induced by the electric field. We defined strain as $\alpha = \Delta L/L$, where L was the size of the sample along the ultrasound axis (z-axis) and ΔL was the change of L induced by the electric field. Detailed study on the amplitude change can be found in our previous work[39].

Fig. 4.2 shows the RF signal at one slow-time instant. A and B represent the echo from the front and rear boundary of the sample, respectively. C represents the second

echo (reverberation) from the front boundary of the tissues based on the fact that the values of both the arrival time and the shifting of C (as will be shown in Fig. 4.3(b)) are double those of A.

The shifting induced by the electric field could be due to two factors: the expansion or contraction of the sample, and the speed of sound change in the sample. This is similar to the shifting of ultrasound signals due to temperature change [32]. We define $\beta = \Delta c/c$, where c is the speed of sound and Δc is the change of c induced by the electric field. For simplicity, we assume that the electric field induces a uniform α and β in the homogeneous samples.

The time shifting at point z inside the sample due to the expansion can be approximated as $\frac{2\alpha z}{c}$. Here we choose the rear surface of the sample to be $z_B = 0$ (as shown in Fig. 4.1), since the rear surface is located on a rigid plastic plate and it will not be displaced by the strain inside the sample. We also assume that the speed of sound in the medium between the sample and the transducer is not affected by the electric field inside the sample. We consider the shifting positive when the echo pulse or speckle is shifted toward the transducer. The time shifting at point z inside the sample due to the change of the speed of sound can be approximated as $S(z) = \frac{2\beta(z_A - z)}{c}$, where z_A is the position of the sample's front surface. Therefore, the total time shifting at point z inside the sample can be expressed as

$$S(z) = \frac{2\alpha z}{c} + \frac{2\beta(z_A - z)}{c}. \tag{4.1}$$

Applying the above equation to the front surface at z_A and the rear surface at $z_B = 0$,

we have

$$S(z_A) = \frac{2\alpha z_A}{c}, and\ S(z_B = 0) = \frac{2\beta z_A}{c}, \tag{4.2}$$

which indicate that the shifting at the front boundary is directly proportional to the strain of the sample. The temporal shifting at the sample's rear boundary, which is fixed spatially on the rigid plastic plate, is directly proportional to the changes in the speed of sound in the sample.

4.5 Preliminary results

The lines in Fig. 4.3(a) show the shifting of the front (dashed) and rear(solid) surfaces of the sample versus slow time. After applying 7 V for $60s$, the displacement at the front boundary($S(z_A)$) is $34ns$, while the displacement at the rear boundary($S(z_B)$) is much smaller, close to zero. Therefore, the sample is expanding toward the transducer during the 60 seconds of 7 V application. Between t_2 and t_3, when the voltage source is turned off, the sample surfaces almost remain at the same position as at t_2. Between t_3 and t_4, when an opposite voltage source (- 7V) is applied, the front surface of the sample continues expanding toward the transducer, but at a much smaller rate than in the case of applying +7 V. In our experiments, the rear surface of the sample is in contact with a rigid plastic plate. Therefore, we can assume that the distance between the rear surface and the transducer is constant. According to Eq. 4.2, the shifting at the rear interface corresponds to the integration of the change in the speed of sound inside the sample. A very small shifting at the rear boundary means there is little change in the speed of sound due to the application of the electric field.

To illustrate the strain induced by the electric field inside the sample, we calculate

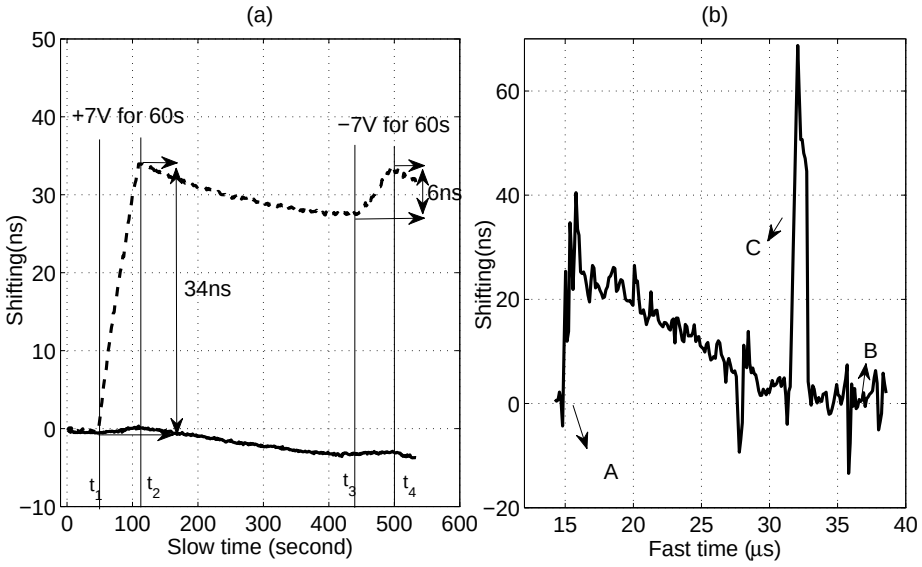

Figure 4.3: (a) Displacement of the front (dashed) and rear(solid) surfaces versus slow time; (b) shifting in the whole sample versus fast time due to the application of 7 Volts for one minute. A, B, and C represents the front boundary of the sample, the rear boundary, and the reverberation from the front boundary, respectively.

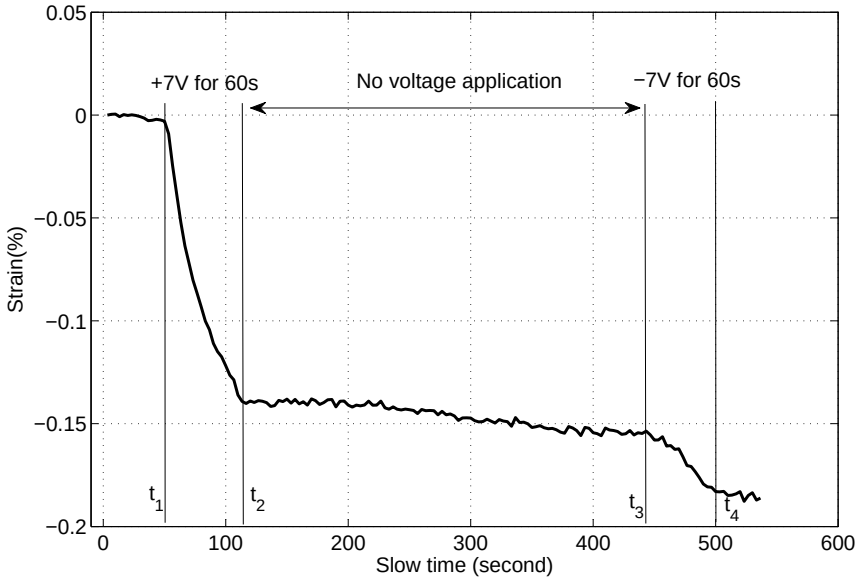

Figure 4.4: Strain versus slow time due to +7V and -7V application.

the shifting between all the corresponding windows of the RF signals at $t_1 = 50s$ (the beginning of applying 7 V) and $t_2 = 110s$ (the end of applying 7 V). Then we plot the shifting versus the fast time (representing the different windows in one RF signal) in Fig. 4.3(b). It clearly shows that a mechanical strain has been induced by the electric field. The magnitude of the strain can be calculated from the graph by using $\alpha = \Delta L/L$.

To study the temporal development of the strain inside the tissue, Fig. 4.4 shows the strain of the sample versus slow time. The strain continuously increases during the $60s$ of applying the positive electric field. After this interval, there is no external field applied and the strain remains at the same level as at the end of applying $7V$. After that, the polarity of the field is reversed. The strain continues increasing until the end of the 60-second application of the negative electric field. The rate of the increase of the strain, however, is much smaller than during the +7 V application.

Similar changes in the arrival time of the ultrasound echoes have also been observed

in various types of tissues such as muscle, kidney, liver, fat, and even gelatin phantoms (3% salt and 10% gel). In all the samples, we have observed that strain can be induced by an applied electric field. But the magnitude of the strain varies among different types of sample, which can be used as a potential method for tissue characterization. The existence this effect in different tissues and gelatin samples indicate that these changes are not due to the contraction of muscle or heart tissues.

4.6 Discussion

Many mechanisms can result in the shifting of ultrasound echoes when an electric field is applied to the samples, such as the piezoelectric effect, tissue contraction, temperature changes due to Joule heating, electrorestriction, and electrokinetic effects such as electrophoresis. Our results exclude Joule heating and electrorestriction as possible mechanisms for the changes in the amplitude and arrival time of the ultrasound echoes, because both Joule heating and electrorestriction are independent of the direction of the electric field. In addition, we will show that the level of changes due to Joule heating is much smaller than that observed in experiments. The rate of the temperature increase for a $7V$ application to the heart muscle tissue is estimated to be 2.5×10^{-3} $^{\circ}C/s$ when assuming the conductivity of heart tissue to be $0.5S/m$. The temperature increase after a one-minute 1.4 V/cm field application is less than 0.15°C and cannot explain the up to $34ns$ shifting observed in the experiments. In another experiment, we measured the temperature rise due to electric field with a thermometer. The results show that there is a temperature rise of less than 0.2°C after applying the $1.6V/cm$ electric field to the heart tissue (with a conductivity of about $0.5S/m$) for four minutes. The temperature rise is a little smaller than the estimated temperature based on assumed adiabatic processes.

This difference can be explained by the thermal conduction between the tissue and the surrounding medium. The strain induced by this temperature rise is much smaller than the strain observed in our experiments.

The piezoelectric effect has been reported for biological tissues. Fig. 4.4 clearly shows that the strain is not due to the piezoelectric effect for three reasons. First, the opposite polarity electric field does not reverse the polarity of the strain. Second, after terminating the field, when there is no field in the sample, the strain does not return to its before-application value. Third, when assuming a piezoelectric coefficient[11] of $2.0pm/V$ the piezoelectric effect can not explain the magnitude of the strain (0.1%) observed in our experiments. The strain due to the piezoelectric effect in biological tissues with the applied electric field of $1.4V/cm$ is estimated to be smaller than 10^{-6}. In addition, the displacement of the tissues in our experiments increases almost linearly with time within the first minute of applying the electric field, which can not be explained by the piezoelectric effect.

It should be pointed out that the positive and negative polarities in applying the electric field are relative. In our experiments, the polarity of the first application of the electric field was chosen randomly, then the polarity of the field was reversed. In all experiments, we found that the strain increases significantly during the first application of the electric field. When the electric field was reversed, the strain increased, however, at a much lower rate in the reported experiments. Therefore, we conclude that the expansion rate depends on the history of applied electric field.

We believe that the electrokinetic effects might be responsible for the changes in the amplitude and arrival time of the ultrasound echoes. As pointed out in the Introduction section, applying an electric field to a colloidal system or to cell cultures can result in electrokinetic effects. The electrokinetic effects have been used to explain the electro-

acoustic phenomena in colloidal system, and changes in shape and orientation of cells and the migration of cells in colloidal/blood and cell cultures when these are subject to an electric field. Therefore it is possible that the strain in the bulk tissues and gelatin phantoms is related to the structural changes in the samples induced by the electrokinetic effects. More detailed comparison between the experimental results and the predictions of the electrokinetics theory is necessary in future studies.

The electrical properties of tissues have been shown to be correlated with their pathological and physiological status by the bio-impedance field[14]. Therefore, it is possible that the electric-field induced changes in tissues, as revealed by changes in the ultrasound echoes, are also correlated with the pathological and physiological status of tissues. So the reported results can potentially lead to a new contrast mechanism for commercial ultrasound imagers: applying a safe level of electric field to subjects and monitoring the changes in ultrasound signals. This is similar to how elastography enriches the information provided by a traditional ultrasound imager. In contrast to the mechanical information provided by elastography, the new technique provides information related to the electrical or electrokinetic properties of tissues at the sonography resolution. Therefore, the new technique could potentially be a novel tissue characterization method at sonography resolution.

4.7 Conclusion

In this paper, we analyze the strain induced in tissues due to the application of an electric field. We found that the sample expands during the application of the electrical field. When the polarity of the applied electric field is reversed, the expansion rate is reduced. The speed of sound changes little compared with the induced strain. Based on these

results, we conclude that temperature rise, piezoelectric effect, tissue contraction and electric restriction can not explain the experimental results. The electrokinetic effects might be one of the underlying mechanisms.

Acknowledgments

This work was supported in part by a Discovery grant from Natural Sciences and Engineering Research Council of Canada (NSERC) and Ryerson Start-up Fund.

Chapter 5

CONCLUSION AND FUTURE WORK

5.1 Conclusion

The preliminary study showed that the effect of physiological-level electric field application to the biomaterial can be observed by using ultrasound echo signals. In this thesis we provided some experimental evidences indicating that electric field induces a strain perpendicular to the applied electric field direction in the tissue. The strain measurement was obtained from the time-shifting of the ultrasound echo signals. Additionally, ultrasound echo amplitude demonstrated some changes correlate with the applied electric field.

To explain changes in specimens, we discussed some possible mechanisms such as piezoelectric effect, electrostriction, Joule heating and electrokinetic effects. Piezoelectric effects and electrostriction were ruled out since they require relatively high electric filed to induce a measurable strain in the tissues. Electrokinetic effects are linearly proportional

with the first power of the applied field strength. This can explain the direction dependent changes in the echo signal. Additionally, induced strain of the sample might be associated with the change in the surface charge density of the tissue cell in a similar way as it was observed due to changing pH value in the tissue[40][16]. Furthermore, electrokinetic effects can be observed for low electric field strength and can be observed for a time interval on the order of seconds. Therefore we believe the mechanism driving these changes possibly associates with the electrokinetic interaction. Further investigations are needed to support this explanation.

In the third chapter, a correlation between the applied electric field and the ultrasound echo signals was presented for some windows in the echo signals. Change in the echo amplitude and echo arrival time were reported by analyzing changes in the peak values in a few windows. Echo amplitude changed depend on the history of the applied electric field. A correlation between the waveform of the applied AC voltage and the derivative of the changes in the amplitude was demonstrated. This is an interesting result since the wave form of the applied electric field can be estimated by processing echo amplitudes.

In chapter four, strain of the tissue were reported from the gradient of the axial shifting. We demonstrated that the shifting along the whole sample has a gradient, which shows a falling trend from the front boundary to the rear boundary of the sample. When we compare the strain for the positive polarity and the negative polarity we observed that the strain depends on the history of the electric field.

5.2 Future work

More future investigations are necessary to advance our understanding of the new effect. One topic of the future studies is the dependence of the new effects on the electrical

properties and mechanical properties of samples. These effects can be investigated on the tissue mimicking phantoms. In a set of experiments, the response can be compared with a varying conductivity or permittivity values of the samples. In other set of experiments, the varying mechanical properties such as water content, can be investigated for constant electrical properties.

Since the motivation behind this study is to develop a new contrast mechanism of ultrasound imaging, more studies are needed in biological samples, for example a sample with layers of fat-muscle tissue. The short term and long term effects, relaxation and saturation responses can be compared between fat and muscle tissues. Although changes observed were in the porcine heart, liver, fat, and muscle tissues and in tissue mimicking phantoms, more studies can be done in tissue characterization by processing changes in the ultrasound echo signals.

References

[1] F. Ahimou, F. A. Denis, A. Touhami, and Y. F. Dufrene. Probing microbial cell surface charges by atomic force microscopy. *American Chemical Society*, 18:9937, 2002.

[2] S. N. Brahmasandra, V. M. Ugaz, and M. A. Burns D. T. Burke, C. H. Mastroangelo. Electrophoresis in microfabricated devices using photopolymerized polyacrylamide gels and electrode-defined sample injection. *Electrophoresis*, 2:300, 2001 Jan.

[3] IEEE Std C95.3-2002(R2008). *IEEE recommended practice for measurements and computations of radio frequency electromagnetic fields with respect to human exposure to such fields, 100kHz-300GHz.* The Institute of Electrical and Electronics Engineers, Inc., New York, June 2008.

[4] N. Chen and A. Chrambach. Enhanced field strength and resolution in gel electrophoresis upon substitution of buffer by histidine at its isoelectric point. *Phys. Med. Biol.*, 17:699, 1996.

[5] P. Debye. A method for the determination of the mass of electrolyte ions. *J. Chem. Phys*, 1:13, 1933.

[6] A.S. Dukhin and P.J. Goetz. *Ultrasound for characterizing colloids*. Elsevier, Amsterdam, 2002.

[7] C. A. Erickson and R. Nuccitelli. Embryonic fibroblast motility and orientation can be influenced by physiological electric fields. *J Cell Biol.*, 1:296, 1984 Jan 1.

[8] E. Ferret, C. Evrard, A. Foucal, and P. Gervais. Volume changes of isolated human k562 leukemia cells induced by electric field pulses. *Biotechnol Bioeng.*, 5:520, 2000 Mar 5.

[9] A. Fontes, H. P. Fernandes, A. A. de Thomaz, L. C. Barbosa, M. L. Barjas-Castro, and C. L. Cesar. Measuring electrical and mechanical properties of red blood cells with double optical tweezers. *J. Biomed. Opt.*, 13:014001, 26 Feb 2008.

[10] S.G. Foster, P.M. Embree, and W.D. O'Brien. Flow velocity profile via time-domain correlation: error analysis and computer simulation. *IEEE Ultrasonics, Ferroelectrics, and Frequency Control Society*, 37:164, May 1990.

[11] E. Fukuda. Piezoelectricity of biopolymers. *Biorheology*, 32:593, Nov. 1995.

[12] S. Grimnes and O. G. Martinsen. *Bioimpedance and Bioelectricity Basics*. Springer Netherlands, San Diego, 2008.

[13] D. Gross, L. M. Loew, and W. W. Webb. Optical imaging of cell membrane potential changes induced by applied electric fields. *Biophys J.*, 2:339, 1986 Aug.

[14] D. Holder. *Electrical impedance tomography: methods, history, and applications*. IOP, London, 2005.

[15] Jyh-Ping Hsu and Aleksandar M. Spasic. *Interfacial Electroviscoelasticity and Electrophoresis*. CRC Press, USA, March 17th 2010.

[16] M. F. Insana, C. P. Barakat, M. Sridhar, and K. K. Lindfors. Viscoelastic imaging of breast tumor microenvironment with ultrasound. *Journal of Mammary Gland Biology and Neoplasia*, 9:393, October 2004.

[17] C. Katnik and R. Waugh. Electric fields induce reversible changes in the surface to volume ratio of micropipette-aspirated erythrocytes. *Biophys J.*, 4:865, 1990 April.

[18] R. Kishi and Y. Osada. Reversible volume change of microparticles in an electric field. *J. Chemical Society*, 85:655, 1989.

[19] P.W. Luther, H.B. Peng, and J.J. Lin. Changes in cell shape and actin distribution induced by constant electric fields. *Nature.*, 61:300, 1983 Nov.

[20] K. J. Mcleod. Microelectrode measurements of low frequency electric field effects in cells and tissues. *Bioelectromag Supp.*, 1:161, 1992.

[21] S. Mthot, V. Moulin, D. Rancourt, M. Bourdages, D. Goulet, M. Plante, F. A. Auger, and L. Germain. Morphological changes of human skin cells exposed to a dc electric field in vitro using a new exposure system. *Canadian journal of chemical engineering*, 79:668, 2001.

[22] E. Neumann, A. E. Sowers, and C. A. Jordan. *Electroporation and electrofusion in cell biology.* Plenum Press, New York, 1989.

[23] M. O'Donnell, A. R. Skovoroda, B. M. Shapo, and S. Y. Emelianov. Internal displacement and strain imaging using ultrasonic speckle tracking. *IEEE Trans. Ultrason. Ferroelect. Freq. Contr.*, 41:314, 1994.

[24] H. Ohshima. Electrophoretic mobility of spherical colloidal particles in concentrated suspensions. *Journal of Colloid and Interface Science*, 188:481, April 1997.

[25] Hiroyuki Ohshima and Kunio Furusawa. *Electrical phenomena at interfaces : fundamentals, measurements, and applications*. New York, New York, c1998.

[26] E. K. Onuma and S. W. Hui. Electric field-directed cell shape changes, displacement, and cytoskeletal reorganization are calcium dependent. *J. Cell Biol.*, 6:2067, 1988 Jun.

[27] J. Ophir, I. Cespedes, H. Ponnekanti, Y. Yazdi, and X. Li. Elastography-a quantitative method for imaging the elasticity of biological tissues. *Ultrason. Imag.*, 13:11, 1991.

[28] J. L. Prince and J. M. Links. *Medical imaging signals and systems*. Pearson Education, Inc., New Jersy, 2006.

[29] P. Prior and B. J. Roth. Electrostriction of anisotropic tissue. *The American Physical Society*, 75:1105, August 2006.

[30] B.J. Rodrigueza, S.V. Kalinina, J. Shina, S. Jessea, V. Grichkod, T. Thundate, A.P. Baddorfa, and A. Gruvermanf. Electromechanical imaging of biomaterials by scanning probe microscopy. *Journal of Structural Biology*, 153:151, February 2006.

[31] G. P. Seehra and F. H. Silver. Viscoelastic properties of acid- and alkaline-treated human dermis: a correlation between total surface charge and elastic modulus. *Skin Research and Technology*, 12:190, 2006.

[32] R. Seip, P. VanBaren, C. A. Cain, and E. S. Ebbini. Noninvasive real-time multipoint temperature control for ultrasound phased array treatments. *IEEE transactions on ultrasonics, ferroelectrics, and frequency control*, 43:1063, Nov. 1996.

[33] S. Sirinivasan and J. Ophir. A zero-crossing strain estimatior for elastography. *Ultrasound in Med. and Biol.*, 29:227, Sep. 2002.

[34] M. Sridhar, D. Huini, C. Pellot-Barakat, J.K. Tsou, and M.F. Insana. Ultrasonic imaging of biochemical changes in tissues. *Ultrasonics Symposium (2004) IEEE*, 3:1051, Aug. 2004.

[35] K. Thethi, P. Jurasz, A. J. MacDonald, A. D. Befus, S.F. Man, and M. J. Duszyk. Determination of cell surface charge by photometric titration. methods. *Journal of Biochemical and Biophysical Methods*, 2:137, 1997 Mar 27.

[36] R. Usha and T. Ramasami. Effect of ph on dimensional stability of rat tail tendon collagen fiber. *Journal of Applied Polymer Science*, 75:1577, 29 July 1999.

[37] D.J. Watmougha, M.B. Shirana, K.M. Quana, A.P. Sarvazyan, E.P. Khizhnyak, and T.N. Pashovkin. Evidence that ultrasonically-induced microbubbles carry a negative electrical charge. *Ultrasonics*, 30:325, 1992.

[38] H. Wen and R.S. Balaban. Ultrasonic imaging of the electroacoustic effect in macromolecular gels. *Ultrason Imaging*, 4:288, 1998 Oct.

[39] Y. Xu and O. Doganay. The effect of electric current in biological tissue on ultrasound echoes. *IEEE International Ultrasonics Symposium*, page 2103, 2009.

[40] R. D. Yapp and M. F. Insana. ph-induced contrast in viscoelasticity imaging of biopolymers. *Phys. Med. Biol.*, 54:1089, 19 December 2008.

[41] U. Zimmermann. Electric field-mediated fusion and related electrical phenomena. *Biochim Biophys*, 3:227, 1982 Nov.